Supporting Information

Photoluminescent ruthenium(II) bipyridyl complexes containing phosphonium ylide ligands

Oussama Fayafrou,[a] Elise Lognon,[b] Carine Duhayon,[a] Jean-Baptiste Sortais,[a] Antonio Monari,*[b] Olivier Baslé,*[a] Yves Canac*[a]

[a] LCC–CNRS, Université de Toulouse, CNRS, UPS, Toulouse, France.

[b] ITODYS, Université Paris Cité and CNRS 75006, Paris, France.

Table of contents

I) General remarks

All manipulations were performed under an inert atmosphere of dry nitrogen by using standard vacuum line and Schlenk tube techniques. Glassware was dried at 120°C in an oven for at least three hours. THF, Et_2O, pentane, toluene and CH_2Cl_2 were dried using an Innovative Technology solvent purification system. Acetonitrile was dried using a MBraun SPS column. Chromatographic purification was carried out on silica gel (SiO_2, 63−200 μm). ^1H, ^{31}P, and ^{13}C NMR spectra were obtained on Bruker AV300, AV400 or NEO600 spectrometers. NMR chemical shifts δ are in ppm, with positive values to high frequency relative to the tetramethylsilane reference for ^1H and ^{13}C, and to H_3PO_4 for ^{31}P. If necessary, additional information on the carbon signal attribution was obtained using $^{13}C\{^1H, ^{31}P\}$, *J*-modulated spin−echo (JMOD) $^{13}C\{^1H\}$, $^1H-^{13}C$ HMQC, and/or HMBC experiments. MS spectra (ESI mode) were performed by the mass spectrometry service of the "Institut de Chimie de Toulouse". Elemental analyses were performed by the elemental analysis service of the LCC-UPR CNRS 8241 with a Perkin Elmer 2400 series II analyzer. Absorption spectra were recorded on PerkinElmer U.V. Spectrometer Lambda 950. Luminescence spectra were obtained with Horiba Jobin Yvon FluoroMax-4 Spectrophotometer. Quantum yield measurements were measured on Hamamatsu spectrometer PL-QY QUANTAURUS QY+. Luminescence lifetimes were recorded on Horiba Fluorolog 3-2iHR320. $[Ru(p\text{-cymene})Cl_2]_2$ was synthetized according literature procedure.[1] All reagent-grade chemicals purchased from commercial sources were used as received.

II) Synthetic procedures

Methyldiphenyl(pyridin-2-yl)phosphonium iodide: 2[I]

Diphenyl-2-pyridylphosphine (1.0 g, 3.8 mmol) and methyl iodide (1.6 g, 11.4 mmol) were dissolved in toluene (40 mL) and the solution was stirred under inert atmosphere at 90 °C for 16 hours. After the toluene was removed, the precipitate was washed with Et_2O (20 mL) and the phosphonium **2**[I] was obtained as a white solid (1.5 g, 98%). Recrystallization from CH_2Cl_2/Et_2O at RT gave colorless crystals suitable for X-ray diffraction analysis. $^{31}P\{^1H\}$ NMR (162 MHz, $CDCl_3$, 25°C): δ 17.1 (s); ^1H NMR (400 MHz, $CDCl_3$, 25°C): δ 8.86 (d, J_{HH} = 4.7 Hz, 1H, CH_{Ar}), 8.11–7.95 (m, 2H, CH_{Ar}), 7.82–7.56 (m, 11H, CH_{Ar}), 3.06 (d, J_{HP} = 13.5 Hz, 3H, CH_3); $^{13}C\{^1H\}$ NMR (101 MHz, $CDCl_3$, 25°C): δ 152.1 (d, J_{CP} = 19.8 Hz, CH_{Py}), 144.3 (d, J_{CP} = 119.7 Hz, C_{Py}), 138.3 (d, J_{CP} = 10.4 Hz, CH_{Py}), 135.2 (d, J_{CP} = 3.1 Hz, CH_{Ph}), 133.4 (d, J_{CP} = 10.5 Hz, CH_{Ph}), 131.2 (d, J_{CP} = 25.1 Hz, CH_{Py}), 130.4 (d, J_{CP} = 13.0 Hz, CH_{Ph}), 128.3 (d, J_{CP} = 3.5 Hz, CH_{Py}), 118.0 (d, J_{CP} = 87.9 Hz, C_{Ph}), 9.8 (d, J_{CP} = 57.2 Hz, CH_3). MS (ES^+): *m/z*: 278.1 $[M - I]^+$; HRMS (ES^+): *m/z*: calculated for $C_{18}H_{17}NP^+$: 278.1099, found: 278.1105, εr =

2.2 ppm. Elemental analysis for $C_{18}H_{17}INP$: calcd, C 53.35, H 4.23, N 3.46; found: C 53.12, H 3.54, N 3.45.

Methyldiphenyl(pyridin-2-yl)phosphonium hexafluorophosphate: 2[PF$_6$]

Phosphonium **2**[I] (0.5 g, 1.2 mmol) was dissolved in CH_2Cl_2/H_2O mixture (1/1) and ammonium hexafluorophosphate (0.3 g, 1.8 mmol) was added to the biphasic solution. The solution was stirred at RT for 2 hours. The organic phase was then separated and dried on Na_2SO_4. After evaporation of the solvent, the desired phosphonium **2**[PF_6] was obtained as a white powder (0.47 g, 90%). Recrystallization from CH_2Cl_2/Et_2O at RT gave colorless crystals suitable for X-ray diffraction analysis. $^{31}P\{^1H\}$ NMR (162 MHz, $CDCl_3$, 25°C): δ 17.0 (s), –144.4 (hept, J_{PF} = 712.7 Hz); ^1H NMR (400 MHz, $CDCl_3$, 25°C): δ 8.88 (d, J_{HH} = 4.7 Hz, 1H, CH_{Ar}), 8.02–7.97 (m, 1H, CH_{Ar}), 7.79–7.74 (m, 3H, CH_{Ar}), 7.72–7.59 (m, 9H, CH_{Ar}), 2.76 (d, J_{HP} = 13.6 Hz, 3H, CH_3); $^{13}C\{^1H\}$ NMR (101 MHz, $CDCl_3$, 25°C): δ 152.3 (d, J_{CP} = 19.9 Hz, CH_{Py}), 144.4 (d, J_{CP} = 119.9 Hz, C_{Py}), 138.3 (d, J_{CP} = 10.4 Hz, CH_{Py}), 135.4 (d, J_{CP} = 3.1 Hz, CH_{Ph}), 133.2 (d, J_{CP} = 10.6 Hz, CH_{Ph}), 130.7 (d, J_{CP} = 25.4 Hz, CH_{Py}), 130.5 (d, J_{CP} = 13.0 Hz, CH_{Ph}), 128.4 (d, J_{CP} = 3.5 Hz, CH_{Py}), 118.1 (d, J_{CP} = 87.8 Hz, C_{Ph}), 7.7 (d, J_{CP} = 59.1 Hz, CH_3). MS (ES^+): *m/z*: 278.1 $[M - PF_6]^+$; HRMS (ES^+): *m/z*: calculated for $C_{18}H_{17}NP^+$: 278.1099, found: 278.1105, εr = 2.2 ppm. Elemental analysis for $C_{18}H_{17}F_6NP_2$: calcd, C 51.08, H 4.05, N 3.31; found: C 50.79, H 3.60, N 3.30.

Ruthenium complex: 3[PF$_6$]

To a solution of **2**[PF_6] (100 mg, 0.23 mmol) in THF (10 mL), KHMDS (0.5 M in toluene, 0.56 mL, 0.28 mmol) was added dropwise at –78 °C under inert atmosphere. The solution was stirred 25 min at –78 °C and then 40 min at –25 °C. This solution was then added to a solution of $[RuCl_2(p\text{-cymene})]_2$ (72 mg, 0.12 mmol) in THF (5 mL) at –78°C and the resulting suspension was stirred at RT for 16 hours. After evaporation of THF, the mixture was dissolved in CH_2Cl_2, filtered over Celite, and the solvent was evaporated. A separation by chromatography column on silica gel was carried out using (80% DCM/20% Acetone) as eluent. The desired complex **3**[PF_6] was obtained as a brown powder (109 mg, 67%). Recrystallization from $MeOH/Et_2O$ at RT gave pale yellow crystals suitable for X-ray diffraction analysis. $^{31}P\{^1H\}$ NMR (162 MHz, CD_3CN, 25°C): δ 48.9 (s); –144.5 (hept, J_{PF} = 707.1 Hz). ^1H NMR (400 MHz, CD_3CN, 25°C): δ 9.51 (d, J_{HH} = 5.6 Hz, 1H, CH_{Ar}), 8.07–8.01 (m, 1H, CH_{Ar}), 7.97–7.88 (m, 1H, CH_{Ar}), 7.84–7.70 (m, 6H, CH_{Ar}), 7.61–7.56 (m, 2H, CH_{Ar}), 7.46–7.40 (m, 3H, CH_{Ar}), 5.59 (s, 2H, p-Cy), 5.47 (d, J_{HH} = 5.7 Hz, 1H, p-Cy), 4.17 (d, J_{HH} = 5.7 Hz, 1H, p-Cy), 3.42 (dd, J_{HH} = 12.8 Hz, J_{HP} = 9.2 Hz, 1H, CH_2), 2.52 (sept, J_{HH} = 6.9 Hz, 1H, CH_{ipr}), 2.16 (dd, J_{HH} = 12.8 Hz, J_{HP} =

10.0 Hz, 1H, CH_2), 1.46 (s, 3H, CH_3), 1.13 (d, J_{HH} = 6.9 Hz, 3H, CH_3), 1.12 (d, J_{HH} = 6.9 Hz, 3H, CH_3); $^{13}C\{^1H\}$NMR (101 MHz, CD_3CN, 25°C): δ 160.6 (d, J_{CP} = 10.2 Hz, CH_{Ar}), 154.1 (d, J_{CP} = 125.2 Hz, C_{Ar}), 140.3 (d, J_{CP} = 8.3 Hz, CH_{Ar}), 136.0 (d, J_{CP} = 2.9 Hz, CH_{Ar}), 135.4 (d, J_{CP} = 3.0 Hz, CH_{Ar}), 133.6 (d, J_{CP} = 11.1 Hz, CH_{Ar}), 133.5 (d, J_{CP} = 10.1 Hz, CH_{Ar}), 133.2 (d, J_{CP} = 19.1 Hz, CH_{Ar}), 131.4 (d, J_{CP} = 12.5 Hz, CH_{Ar}), 131.0 (d, J_{CP} = 11.9 Hz, CH_{Ar}), 130.9 (d, J_{CP} = 2.0 Hz, CH_{Ar}), 126.1 (d, J_{CP} = 68.3 Hz, C_{Ar}), 120.9 (d, J_{CP} = 88.8 Hz, C_{Ar}), 101.8 (s, C_{Ar}), 98.8 (s, C_{Ar}), 92.6 (s, CH_{Ar}), 89.1 (s, CH_{Ar}), 85.3 (s, CH_{Ar}), 80.0 (s, CH_{Ar}), 31.7 (s, CH_{ipr}), 23.5 (s, CH_3), 21.7 (s, CH_3), 18.1 (s, CH_3), 0.3 (d, J_{CP} = 31.3 Hz, CH_2). MS (ES^+): *m/z*: 548.1 [M – PF_6]$^+$; HRMS (ES^+): *m/z*: calculated for $C_{28}H_{30}NClPRu^+$: 548.0848, found: 548.0854, εr = 1.1 ppm. Elemental analysis for $C_{28}H_{30}ClF_6NP_2Ru$: calcd, C 48.53, H 4.36, N 2.02; found: C 48.39, H 3.68, N 2.08.

Ruthenium complex: C[PF_6]$_2$

Ru complex **3**[PF_6] (100 mg, 0.14 mmol) and 2,2'-bipyridyl (45 mg, 0.28 mmol) were dissolved in DMSO (2 mL). The mixture was stirred at RT for 5 min under inert atmosphere. To this mixture, a solution of $AgPF_6$ (43 mg, 0.17 mmol) in DMSO (1 mL) was added dropwise, and the mixture was heated to 130 °C for 16 hours protected from light. The color of the mixture changed from orange to dark red. The mixture was then cooled to RT and added dropwise to 10 mL of cold Et_2O affording a dark red precipitate. After evaporation of the DMSO via trap-to-trap distillation, a separation by chromatography column on silica gel was carried out using (90% DCM/10% Acetone) as eluent. The desired complex **C**[PF_6]$_2$ was obtained as a dark red powder (127 mg, 90%). Recrystallization from CH_2Cl_2/Et_2O at RT gave dark red crystals suitable for X-ray diffraction analysis. $^{31}P\{^1H\}$ NMR (162 MHz, CD_3CN, 25°C): δ 45.4 (s); –144.6 (hept, J_{PF} = 707.1 Hz). ^1H NMR (400 MHz, CD_3CN, 25°C): δ 9.12 (d, J_{HH} = 5.7 Hz, 1H, CH_{Ar}), 8.59 (d, J_{HH} = 8.2 Hz, 1H, CH_{Ar}), 8.51 (t, J_{HH} = 8.0 Hz, 2H, CH_{Ar}), 8.29 (dd, J_{HH} = 13.1, 8.1 Hz, 2H, CH_{Ar}), 8.15 (t, J_{HH} = 8.0 Hz, 1H, CH_{Ar}), 8.06 (t, J_{HH} = 7.9 Hz, 1H, CH_{Ar}), 7.96 (t, J_{HH} = 7.8 Hz, 1H, CH_{Ar}), 7.90–7.65 (m, 9H, CH_{Ar}), 7.64–7.57 (m, 2H, CH_{Ar}), 7.56 (d, J_{HH} = 5.6 Hz, 1H, CH_{Ar}), 7.47–7.34 (m, 5H, CH_{Ar}), 7.31–7.27 (m, 2H, CH_{Ar}), 7.16 (t, J_{HH} = 7.1 Hz, 1H, CH_{Ar}), 6.65 (t, J_{HH} = 7.2 Hz, 1H, CH_{Ar}), 1.81 (dd, J_{HH} = 14.6 Hz, J_{HP} = 9.0 Hz, 1H, CH_2), 0.87 (dd, J_{HH} = 14.6 Hz, J_{HP} = 12.5 Hz, 1H, CH_2); ^{13}C NMR (101 MHz, CD_3CN, 25°C): δ 160.4 (d, J_{CP} = 127.7 Hz, C_{Ar}), 158.9 (s, C_{Ar}), 157.9 (s, C_{Ar}), 157.8 (s, C_{Ar}), 157.7 (s, C_{Ar}), 157.5 (s, C_{Ar}), 155.6 (d, J_{CP} = 9.3 Hz, CH_{Ar}), 152.6 (s, CH_{Ar}), 152.5 (s, CH_{Ar}), 152.4 (s, CH_{Ar}), 152.1 (s, CH_{Ar}), 150.8 (s, CH_{Ar}), 138.7 (s, CH_{Ar}), 138.0 (s, CH_{Ar}), 137.7 (s, CH_{Ar}), 137.1 (d, J_{CP} = 8.8 Hz, CH_{Ar}), 136.6 (s, CH_{Ar}), 136.4 (s, CH_{Ar}), 135.0 (d, J_{CP} = 6.1 Hz, CH_{Ar}), 134.9 (d, J_{CP} = 18.2 Hz, CH_{Ar}), 134.8 (d, J_{CP} = 6.1 Hz, CH_{Ar}), 133.1 (d, J_{CP}

= 10.8 Hz, CH_{Ar}), 133.0 (d, J_{CP} = 9.9 Hz, CH_{Ar}), 131.2 (d, J_{CP} = 12.2 Hz, CH_{Ar}), 130.9 (d, J_{CP} = 11.8 Hz, CH_{Ar}), 130.0 (d, J_{CP} = 2.5 Hz, CH_{Ar}), 128.5 (s, CH_{Ar}), 128.2 (d, J_{CP} = 64.6 Hz, C_{Ar}), 128.0 (s, CH_{Ar}), 127.0 (s, CH_{Ar}), 126.9 (s, CH_{Ar}), 125.4 (s, CH_{Ar}), 125.2 (s, CH_{Ar}), 125.0 (s, CH_{Ar}), 124.4 (s, CH_{Ar}), 124.1 (s, CH_{Ar}), 121.6 (d, J_{CP} = 82.1 Hz, C_{Ar}), –0.2 (d, J_{CP} = 20.6 Hz, CH_2). MS (ES^+): *m/z*: 836.1 $[M - PF_6]^+$; HRMS (ES^+): *m/z*: calculated for $C_{38}H_{32}N_5P_2RuF_6^+$: 836.1081, found: 836.1104, εr = 2.8 ppm. Elemental analysis for $C_{38}H_{32}F_{12}N_5P_3Ru.(CH_2Cl_2)$: calcd, C 43.96, H 3.22, N 6.57; found: C 44.18, H 2.96, N 6.54.

Ruthenium complex: 4[PF_6]$_2$

To a solution of Ru complex **3**[PF_6] (100 mg, 0.14 mmol) in CH_3CN (5 mL), $AgPF_6$ (55 mg, 0.21 mmol) was added, and the mixture was heated to 100 °C for 16 hours. After evaporation of CH_3CN, the mixture was dissolved in CH_2Cl_2 (5 mL), filtered over Celite, and the solvent was evaporated. A DCM/Et_2O precipitation was carried out and the desired product **4**[PF_6]$_2$ was obtained as a yellowish green powder (114 mg, 95%). Recrystallization from CH_2Cl_2/Et_2O at RT gave yellow crystals suitable for X-ray diffraction analysis. $^{31}P\{^1H\}$ NMR (162 MHz, CD_2Cl_2, 25°C): δ 48.8 (s); –144.5 (hept, J_{PF} = 707.1 Hz). ^1H NMR (400 MHz, CD_2Cl_2, 25°C): δ 9.29 (d, J_{HH} = 5.6 Hz, 1H, CH_{Ar}), 7.95–7.90 (m, 1H, CH_{Ar}), 7.81–7.62 (m, 7H, CH_{Ar}), 7.57–7.47 (m, 4H, CH_{Ar}), 7.35 (t, J_{HH} = 6.8 Hz, 1H, CH_{Ar}), 2.54 (s, 3H, CH_3), 2.48 (s, 3H, CH_3), 2.02 (s, 6H, CH_3), 1.91 (d, J_{HP} = 9.2 Hz, 2H, CH_2).^{13}C NMR (101 MHz, CD_2Cl_2, 25°C) : δ 159.1 (d, J_{CP} = 127.0 Hz, C_{Ar}), 158.3 (d, J_{CP} = 8.8 Hz, CH_{Ar}), 137.1 (d, J_{CP} = 8.6 Hz, CH_{Ar}), 134.6 (d, J_{CP} = 3.0 Hz, CH_{Ar}), 132.9 (d, J_{CP} = 18.2 Hz, CH_{Ar}), 132.6 (d, J_{CP} = 10.2 Hz, CH_{Ar}), 130.5 (d, J_{CP} = 11.9 Hz, CH_{Ar}), 129.1 (d, J_{CP} = 2.4 Hz, CH_{Ar}), 125.6 (s, C_{CN}), 125.1 (s, C_{CN}), 124.7 (d, J_{CP} = 76.4 Hz, C_{Ar}), 121.9 (s, C_{CN}), 4.2 (s, CH_3), 3.8 (s, CH_3), 3.7 (s, CH_3), –9.9 (d, J_{CP} = 24.7 Hz, CH_2). MS (ES^+): *m/z*: 688.1 $[M - PF_6]^+$; HRMS (ES^+): *m/z*: calculated for $C_{26}H_{28}N_5P_2RuF_6^+$: 688.0775, found: 688.0778, εr = 0.4 ppm.

III) X-Ray Diffraction

Single crystals suitable for X-ray diffraction were coated with paratone oil and mounted on the goniometer. The X-ray crystallographic data were obtained at 100 K from a RIGAKU Synergy diffractometer (CuKα radiation source) equipped with an Oxford Cryosystem. The structures have been solved by direct methods using SHELXT[2] or SUPERFLIP[3] and refined by means of least-square procedures on F^2 using CRYSTALS.[4] The scattering factors for all the atoms were used as listed in the International Tables for X-ray Crystallography.[5] Absorption correction was performed using a multi-scan procedure. All non-hydrogen atoms were refined anisotropically excepting for **4**[PF_6]$_2$ (a half occupancy CH_3CN was isotropically refined). For

this structure, the PF_6 anion was disordered over 2 positions. Restraints were applied to this model. For **2**[PF_6], the N atom of the pyridyl was found to be disordered over 6 positions with occupancies varying from 0.08 to 0.40. Refinement of the final model led to an imperfect but reasonable solution and confirmed the structure. The detected electron densities suggested the presence of highly disordered solvent molecules, therefore we decided to remove this residual density using the SQUEEZE facility from PLATON.[6] The H atoms were usually located in a difference map, but those attached to carbon atoms were systematically repositioned geometrically. The H atoms were initially refined with soft restraints on the bond lengths and angles to regularize their geometry and Uiso (H) (in the range 1.2-1.5 times Ueq of the parent atom), after which the positions were refined with riding constraints. Crystallographic information for all the complexes is gathered in Table S1; the CIF files are also available from the Cambridge Crystallographic Data Centre (www.ccdc.cam.ac.uk/data_request/cif) under the references CCDC 2382356-2382360.

Table S1. Crystallographic information for **2**[I], **2**[PF_6], **3**[PF_6], **C**[PF_6]$_2$ and **4**[PF_6]$_2$.

	2[I]	**2**[PF_6]	**3**[PF_6]	**C**[PF_6]$_2$	**4**[PF_6]$_2$
Formula	$C_{18}H_{17}INP$	$C_{18}H_{17}F_6NP_2$	$C_{28}H_{30}ClF_6NP_2Ru$	$C_{39}H_{34}Cl_2F_{12}N_5P_3Ru$	$C_{27}H_{30.50}F_{12}N_{5.5}O_{0.5}P_3Ru$
M_w (g mol^{-1})	405.22	423.28	693.01	1065.60	862.55
T (K)	100	100	100	100	100
Crystal system	orthorhombic	monoclinic	monoclinic	triclinic	triclinic
Space group	P bca	C 2/c	P 2$_1$/n	P -1	P -1
a (Å)	12.63127(6)	24.3853(6)	10.9068(1)	11.9812(1)	11.9873(1)
b (Å)	12.19906(5)	12.6612(1)	15.3075(1)	13.8864(1)	12.2991(1)
c (Å)	22.48435(10)	13.1682(1)	17.2234(1)	14.5882(2)	13.4048(1)
α (°)	90	90	90	95.300(1)	100.976(1)
β (°)	90	98.506(2)	92.768(1)	110.311(1)	100.112(1)
γ (°)	90	90	90	92.430(1)	106.324(1)
V (Å^3)	3464.60(3)	4020.92(11)	2872.19(4)	2259.26(4)	1806.06(3)
Z	8	8	4	2	2
$\rho_{calcd.}$ (g cm^{-3})	1.554	1.398	1.603	1.566	1.583
μ (mm^{-1})	15.33	2.497	6.852	5.665	5.611
Collected reflns	116235	76149	125616	126017	12159
Unique reflns	3786	4154	5956	9706	7348
R_{int}	0.062	0.043	0.057	0.090	0.014
Nb of parameters	190	244	352	586	442
Nb of reflns($I \geq 2\sigma$)	3498	3857	5532	8193	6856
Refinement on	F^2	F^2	F^2	F^2	F^2
Final *R*, *wR* ($I \geq 2\sigma$)	0.0341, 0.0952	0.0326, 0.0875	0.0240, 0.0669	0.0705, 0.2035	0.0741, 0.1946
R, *wR* (all data)	0.0343, 0.0955	0.0329, 0.0878	0.0244, 0.0674	0.0728, 0.2065	0.0748, 0.1953
$\Delta\rho_{min}$/ $\Delta\rho_{max}$	-1.09/2.63	0.41/-0.39	-0.64/0.59	-1.01/2.27	-2.12/2.77
CCDC Dep. Number	2382356	2382357	2382358	2382359	2382360

IV) Photophysical experiments

1) UV-Vis and photoluminescence spectra

Absorption spectra were recorded on PerkinElmer U.V. Spectrometer Lambda 950, in a quartz cuvette (10x10 mm light path) with a screw-cap, in degassed CH_2Cl_2, at 1.10^{-5} M with a scan range of 800 nm to 250 nm at a scan rate of 250 nm/min at room temperature.

Luminescence spectra were obtained with Horiba Jobin Yvon FluoroMax-4 Spectrophotometer, in a quartz cuvette (10x10 mm light path) with a screw-cap, in degassed CH_2Cl_2, at 1.10^{-5} M, at room temperature, with a spectral window from 500 nm to 900 nm, an excitation wavelength at 495 nm, an increment of 1.00 nm and an integration time of 0.10 s. Luminescence in the solid state were measured at 273 K (Figure S1) and at 77 K (Figure S2).

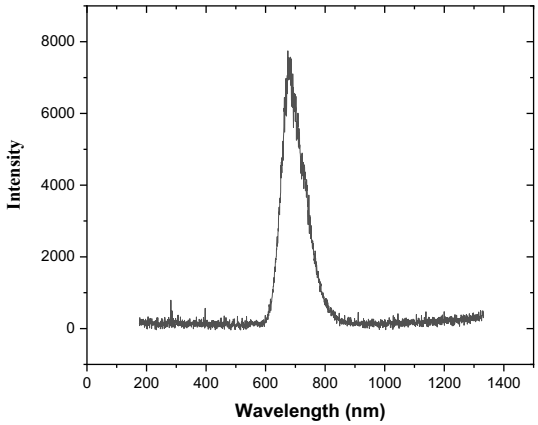

Figure S1. Emission spectrum of **C**$[PF_6]_2$ in the solid state at 273 K.

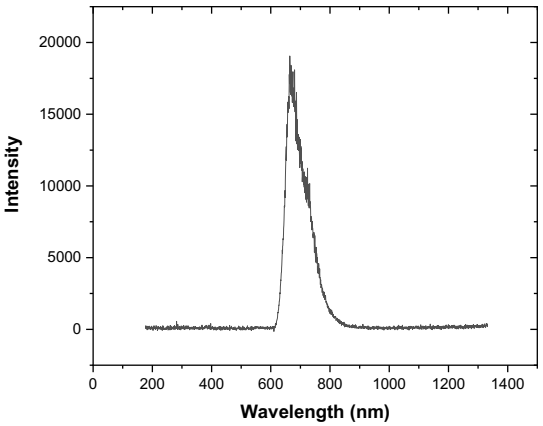

Figure S2. Emission spectrum of **C**$[PF_6]_2$ in the solid state at 77 K.

2) Excited state lifetimes

Luminescence lifetimes were recorded on Horiba Fluorolog 3-2iHR320 equipped with the NanoLED module for TCSPC (Time Correlated Single Photon Counting) lifetime measurements. Samples were excited with a λ = 455 nm NanoLED. Emission was recorded at 672 nm, with a measurement range of 13 microseconds and with a max signal bellow than 2.00%. A 0.01% solution of LUDOX AS-40 colloidal silica (40 wt. % suspensions in H_2O) in purified water was used as reference. Photocatalyst solution were prepared with a concentration around 10^{-5} M in CH_2Cl_2 and placed in a quartz cuvette (10x10 mm light path) with a screw-cap. Samples were degassed for 10 minutes to remove oxygen and avoid the triplet excited-state quenching. The software DAS 6 was used to perform a monoexponential fitting analysis to calculate the lifetimes (Figure S3).

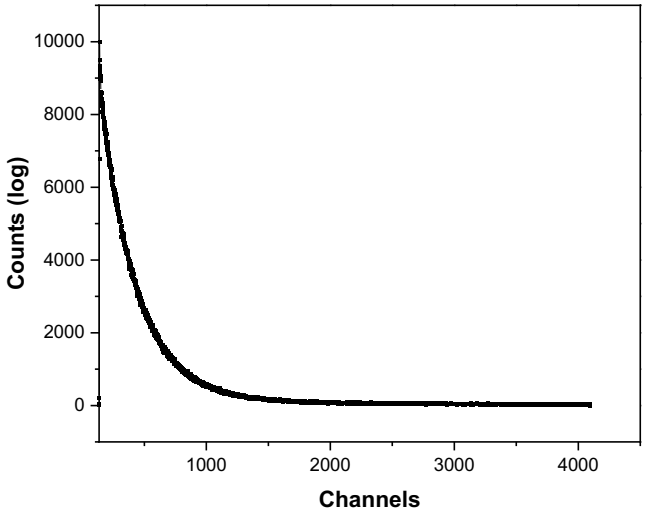

Figure S3. Excited-state life time of **C**$[PF_6]_2$ in CH_2Cl_2.

3) Luminescence quantum yields

Quantum yield measurements were measured on Hamamatsu spectrometer PL-QY QUANTAURUS QY+. Samples were prepared with a concentration of 1.10^{-5} M in CH_2Cl_2 and placed in 1 ml cylindrical glass cuvette. The solution was degassed directly into the cuvette for 2.5 min just before the analysis.

4) Photostability

After fixing the absorbance of the MLCT band to 1, a solution of [**C**]$(PF_6)_2$ or $[Ru(bpy)_3](PF_6)_2$ in degassed CH_2Cl_2 was introduced in a quartz cuvette (10x10 mm light path) with a screw-cap. Emission spectra were recorded with Horiba Jobin Yvon FluoroMAx-4

Spectrophotometer, with a spectral window from 500 nm to 900 nm, an excitation wavelength at 495 nm. Luminescence spectra were recorded to estimate the maximum intensity I_0 at t = 0. Then, the sample was irradiated with blue LED in the photoreactor (λ = 460 nm) and the decreasing of luminescence was measured at t = x minutes (Tables S2-S3). The ratio between I and I_0 was calculated for each point to draw the graph for complex [**C**]$(PF_6)_2$ (Figure S4).

	t = 0 min	t = 6 min	t = 16 min	t = 28 min	t = 48 min	t = 60 min
Measurement	1067070	1007830	924740	902290	874320	825580
I/I_0	1	0.95	0.90	0.85	0.82	0.79

Table S2. Values of photostability experiment for [**C**]$(PF_6)_2$.

	t = 0 min	t = 10 min	t = 20 min	t = 30 min	t = 40 min	t = 60 min
Measurement	17360820	16650560	16424440	16141620	16089160	15772210
I/I_0	1	0.95	0.94	0.929	0.926	0.90

Table S3. Values of photostability experiment for $[Ru(bpy)_3](PF_6)_2$.

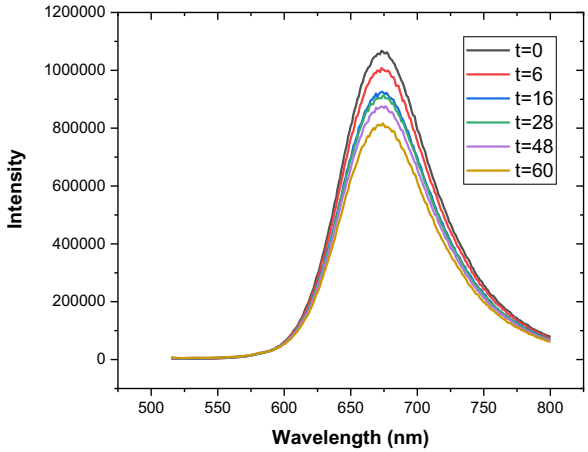

Figure S4. Luminescence decrease for [**C**]$(PF_6)_2$ after irradiation at 460 nm in CH_2Cl_2.

V) Electrochemical data

Voltammetric measurements were carried out with a potentiostat Autolab PGSTAT100 controlled by GPES 4.09 software. Experiments were performed at RT in a homemade airtight three-electrode cell consisting of a Pt working electrode (d = 0.5 mm), a platinum wire (S = 1 cm^2) as counter electrode, and a saturated calomel electrode (*SCE*) separated from the solution by a bridge compartment as a reference. Before each measurement, the working electrode was

cleaned with a polishing machine (Presi P230, P4000). The measurements were carried out in dry CH_2Cl_2 under argon atmosphere using 0.1 M [nBu$_4$N](PF$_6$) (Fluka, 99% puriss electrochemical grade) as supporting electrolyte and typically 10^{-3} M sample concentration.

	E_{00} (eV)[a]	$E^{1/2}(Ru^{2+/3+})$ (V)[b]	$E^{1/2}(Ru^{2+/+})$ (V)[b]	$E(Ru^{2+*/3+})$ (V)	$E(Ru^{2+*/+})$ (V)
[**C**](PF$_6$)$_2$	1.84	0.95	–1.46	–0.89	0.38

[a] E_{00} was estimated from the λ_{max} values on emission spectra in CH_2Cl_2.
[b] Redox potentials (V) are given vs saturated calomel electrode (SCE).

Table S4. Ground-state and excited-state redox potentials for [**C**](PF$_6$)$_2$ in CH_2Cl_2.

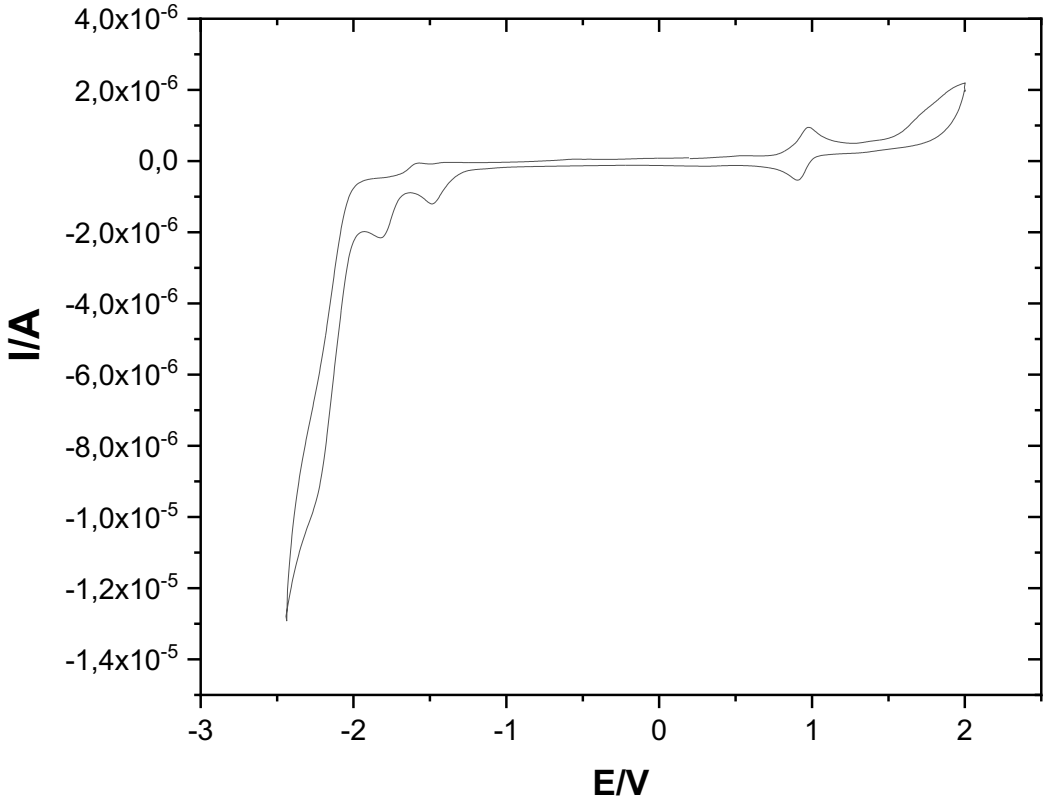

Figure S5. Cyclic voltammogram of [**C**](PF$_6$)$_2$ in CH_2Cl_2 (sweep rate = 200 mV/s).

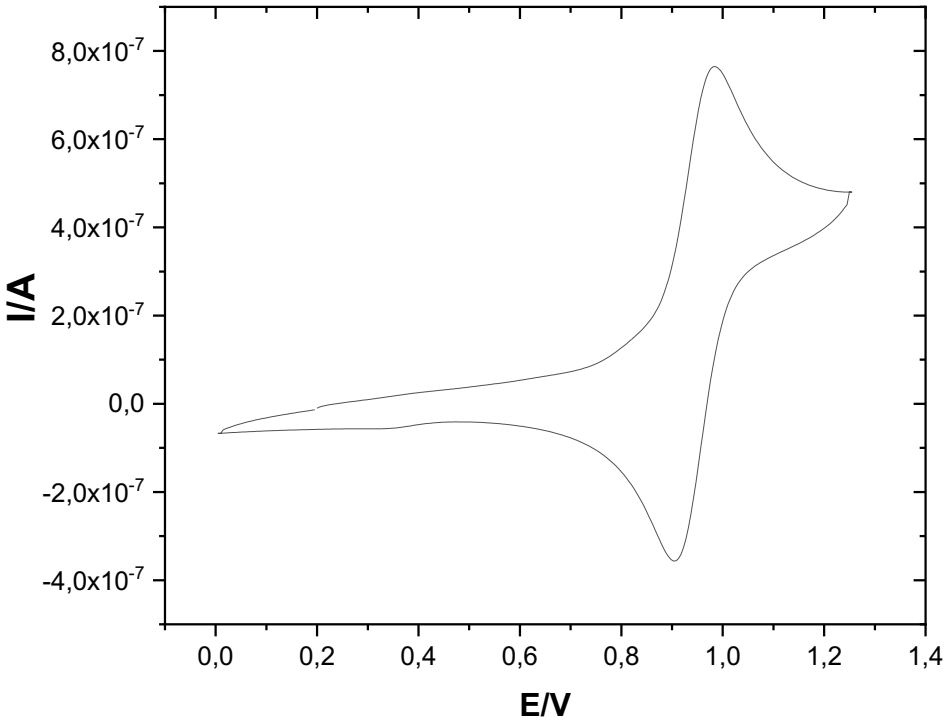

Figure S6. Zoom on oxidation potentials for [**C**]$(PF_6)_2$ in CH_2Cl_2.

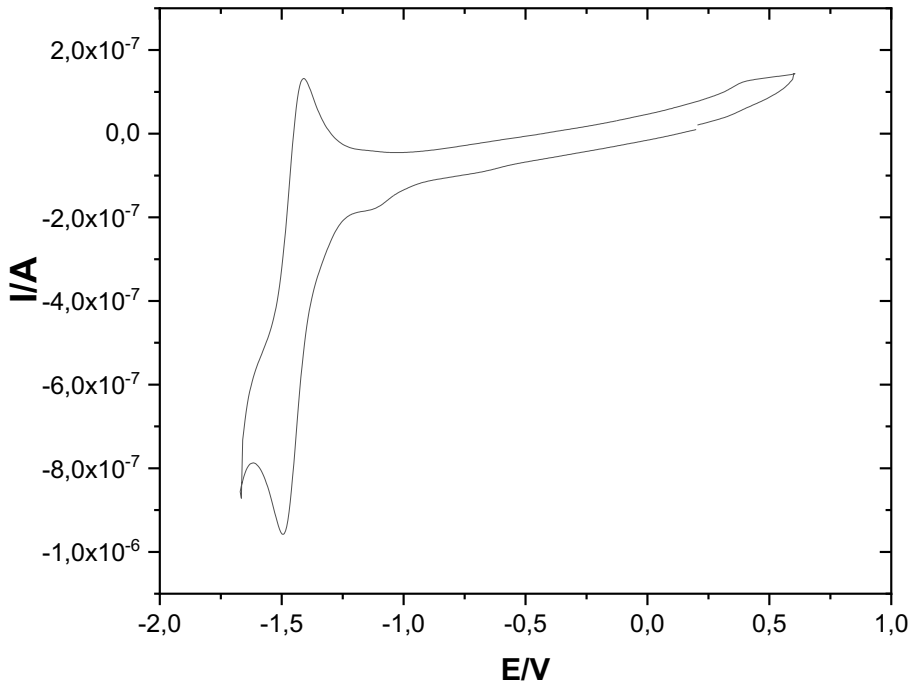

Figure S7. Zoom on reduction potentials for [**C**]$(PF_6)_2$ in CH_2Cl_2.

VI) Catalytic procedures

General procedure: Aza-Henry reaction

To a flame-dried 5 mL vial was added Ru catalyst (0.01 equiv), tetrahydroisoquinoline (0.2 mmol, 1.0 equiv), and nitromethane degassed with O_2 (1 mL). The reaction mixture was stirred at RT under O_2 atmosphere for selected time and at a distance of ~5 cm from a 26 W fluorescent lamp of 460 nm. After filtration over Celite and evaporation of the solvent, the residue was directly analyzed by ^{1}H NMR. The conversion yields were calculated by integrating the peaks in the ^{1}H NMR spectrum using 1,3,5-trimethoxybenzene as internal standard.

General procedure: Photoisomerization of *E*-stilbene

To a flame-dried 5 mL vial was added Ru catalyst (0.01 equiv), *E*-stilbene (0.2 mmol, 1.0 equiv), and nitromethane degassed with argon (1 mL). The reaction mixture was stirred at RT under argon atmosphere for selected time at a distance of ~5 cm from a 26 W fluorescent lamp of 460 nm. After filtration over Celite and evaporation of the solvent, the residue was directly analyzed by ^{1}H NMR. The conversion yields were calculated by integrating the peaks in the ^{1}H NMR spectrum using 1,3,5-trimethoxybenzene as internal standard.

VII) Computational studies

Molecular modeling was performed at the density functional theory (DFT) level using consistently the ORCA 4.2.1 code.[7,8] Singlet ground state geometry optimization was performed with the B3LYP exchange-correlation functional[9] adding Grimme dispersion corrections, while the Def2-SVP basis set was used consistently for all the Ru bipyridyl complexes [**A**], [**B**], and [**C**]. Dichloromethane solvent was implicitly taken into account in all calculations using the Polarizable Continuum Model (PCM)[10] as implemented in ORCA 4. The absorption spectra were obtained from the 30 lowest vertical excitation energy obtained at Franck-Condon at Time Dependent DFT (TD-DFT) level using CAM-B3LYP exchange-correlation functional[11] with the Def2-SVP basis set. To better compare the experimental results, the vertical transitions have been convoluted with a Gaussian function of maximum-width at half-height of 0.3 eV. Natural Transition Orbitals (NTO)[12] have been used to identify the electronic nature of the different states. The lowest singlet excited state S1, has been optimized at the TD-DFT level, while the lowest triplet state T1, has been optimized as the ground state for its specific spin multiplicity, and its nature has been identified considering the spin density. The same protocol has been used for the calculation of the redox properties of [**C**] optimizing either the oxidized or the reduced species. For the calculation of the energy transfer of [**C**] with stilbene, each system has been optimized in its respective ground state and first

triplet state using the CAM-B3LYP exchange-correlation functional and the Def2-SVP basis set. An energetic penalty of 7.2 kcal/mol was found for the isomerization of *E*-stilbene which might be overcome by vibronic coupling.[13]

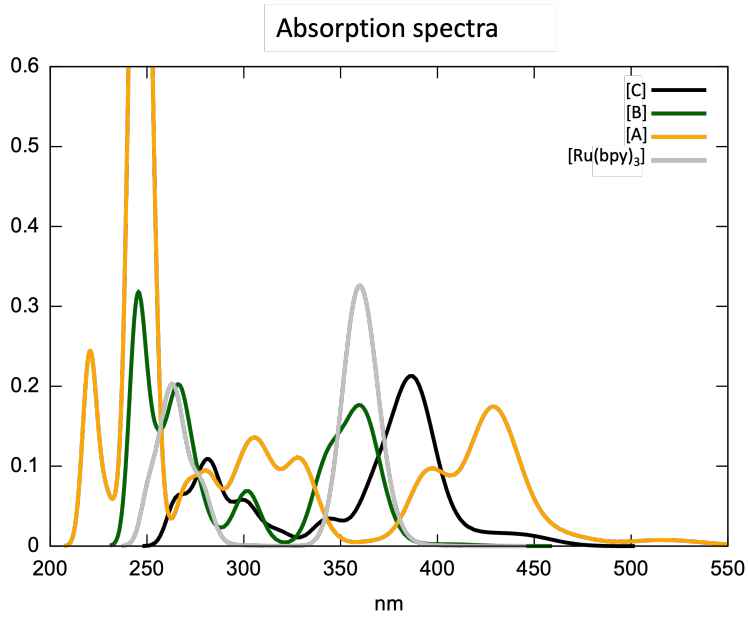

Figure S8. Simulated TD-DFT absorption spectra of complexes [**A**], [**B**], [**C**] and [Ru(bpy)$_3$].

complex	λ_{abs} (nm)	f	Electronic nature
[**C**]	283, 388	0.04, 0.16	MLCT
[**B**]	269, 302, 362	0.05, 0.06, 0.16	MLCT
[**A**]	245, 311, 397, 429	0.68, 0.05, 0.08, 0.17	MLCT
[Ru(bpy)$_3$]	260, 358, 361	0.05, 0.15, 0.17	MLCT

Table S5. Principal vertical transition, oscillator strength, and their nature.

complex	S1→S0 (eV)	T1→S0 (eV)	ΔMC/MLCT (eV)
[**C**]	1.91	1.43	0.42
[**B**]	2.02	1.77	1.02
[**A**]	1.61	1.28	1.67
[Ru(bpy)$_3$]	2.40	1.62	1.02

Table S6. Vertical transition energies from the excited state, either S1 or T1, equilibrium geometry towards the ground state S0. The MC/MLCT gap at Franck Condon is also given.

VIII) NMR spectra

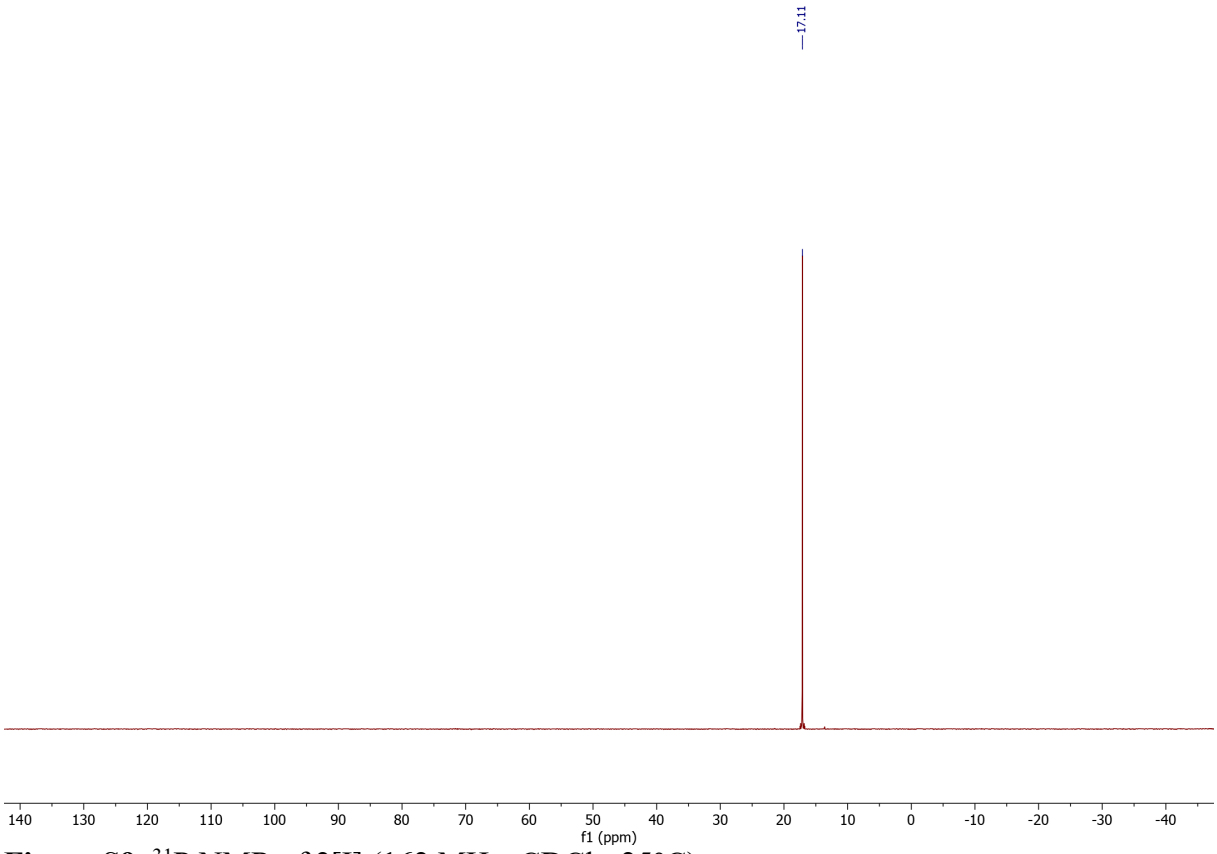

Figure S9. ^{31}P NMR of **2**[I] (162 MHz, $CDCl_3$, 25°C)

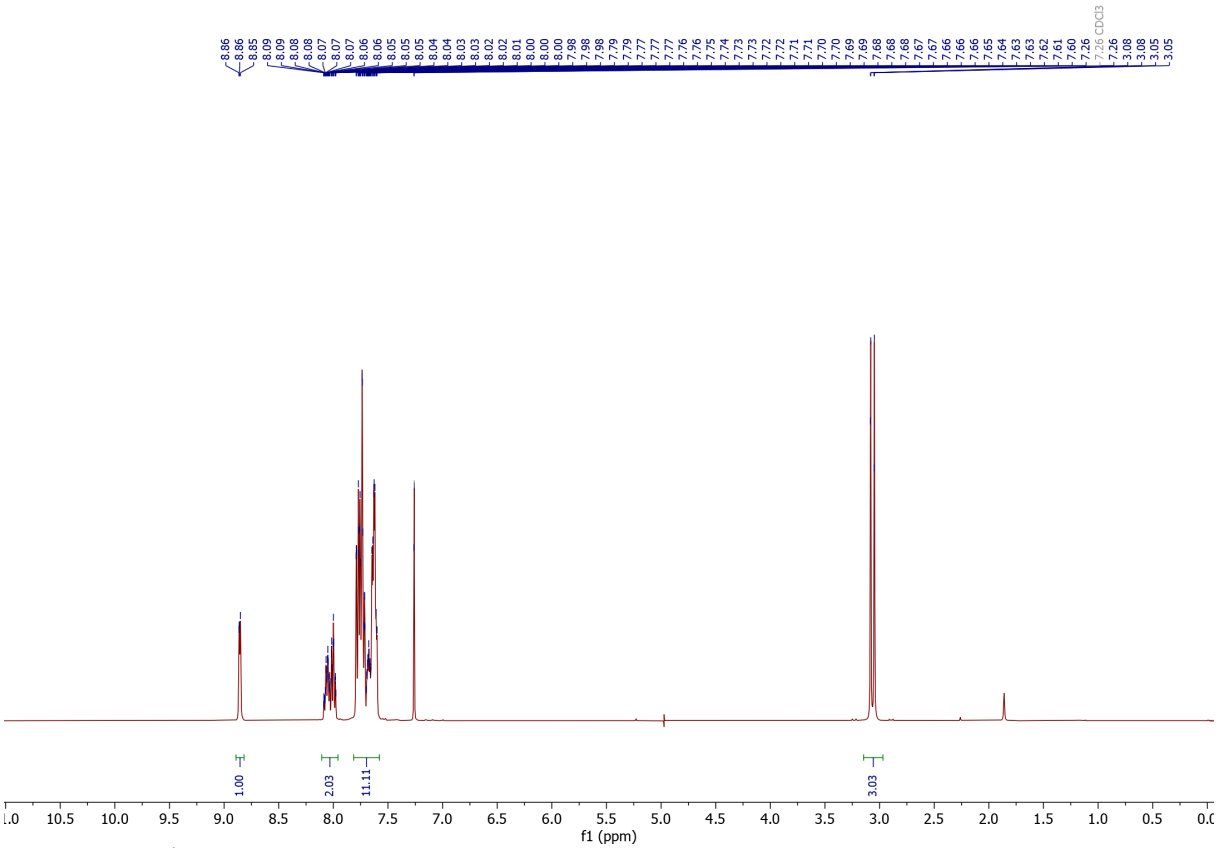

Figure S10. ^{1}H NMR of **2**[I] (400 MHz, $CDCl_3$, 25°C)

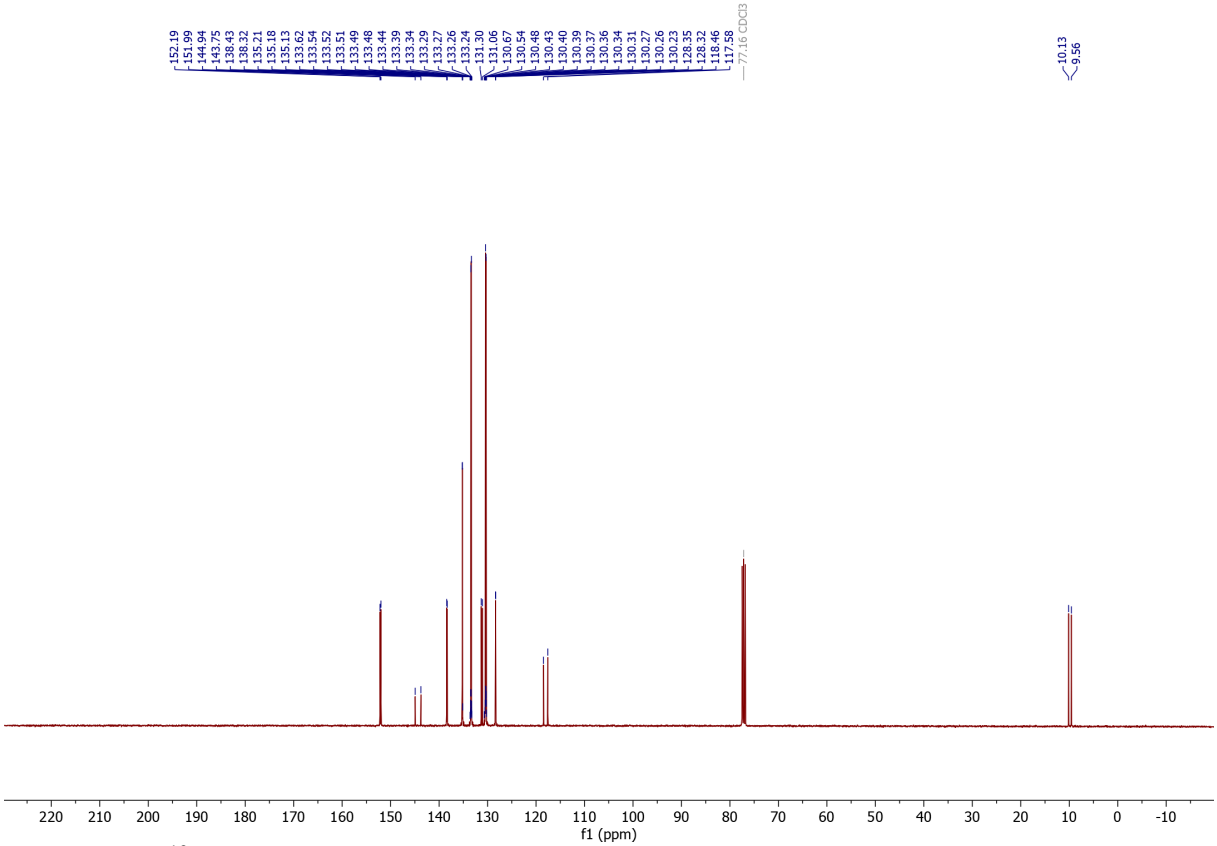

Figure S11. ^{13}C NMR of **2**[I] (101 MHz, $CDCl_3$, 25°C)

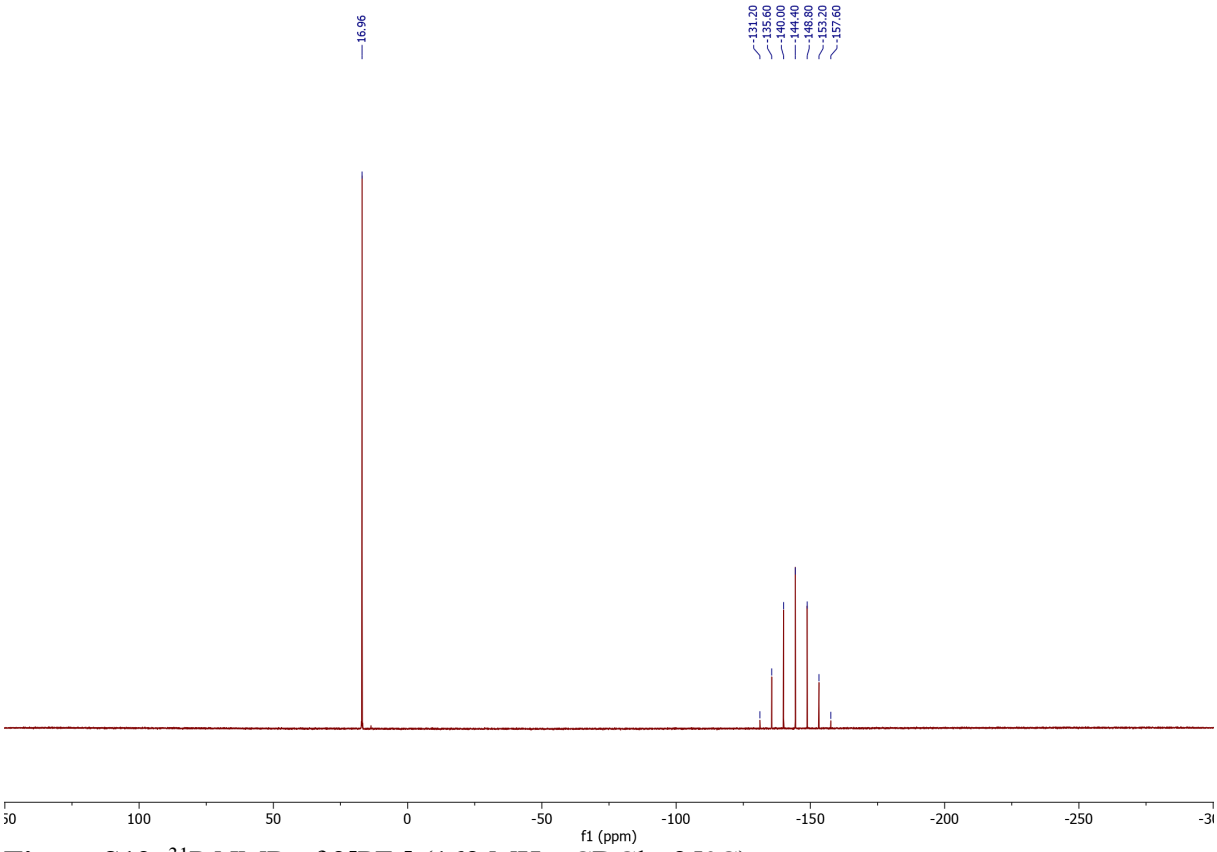

Figure S12. ^{31}P NMR of **2**[PF_6] (162 MHz, $CDCl_3$, 25°C)

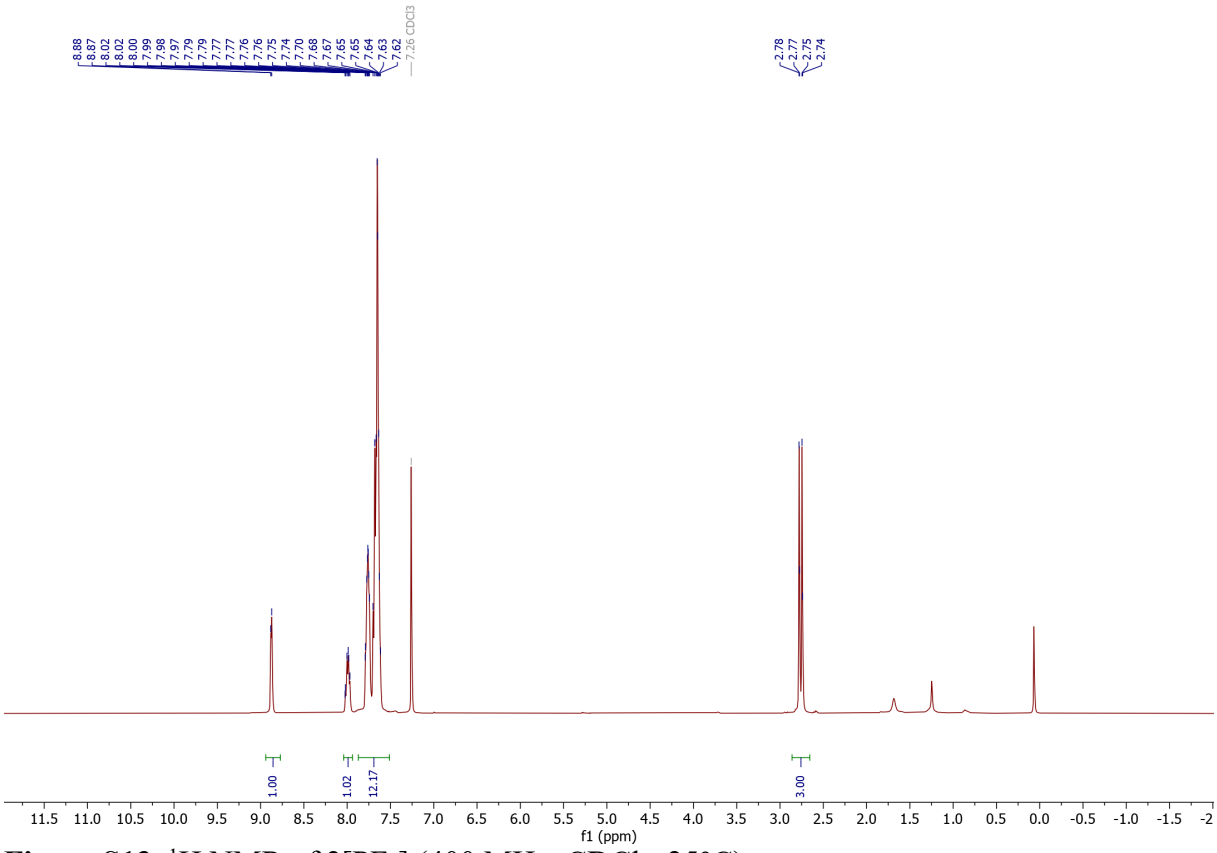

Figure S13. ^{1}H NMR of **2**[PF_6] (400 MHz, $CDCl_3$, 25°C)

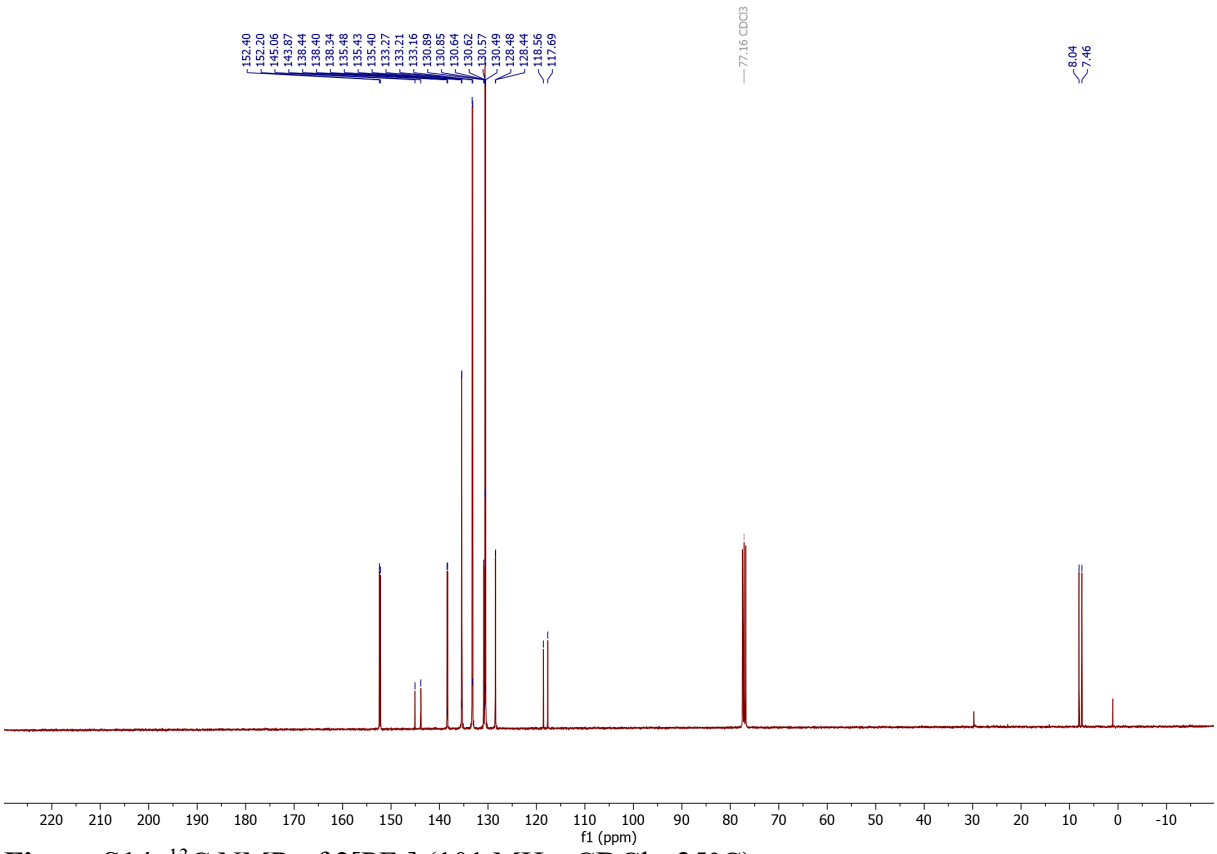

Figure S14. ^{13}C NMR of **2**[PF_6] (101 MHz, $CDCl_3$, 25°C)

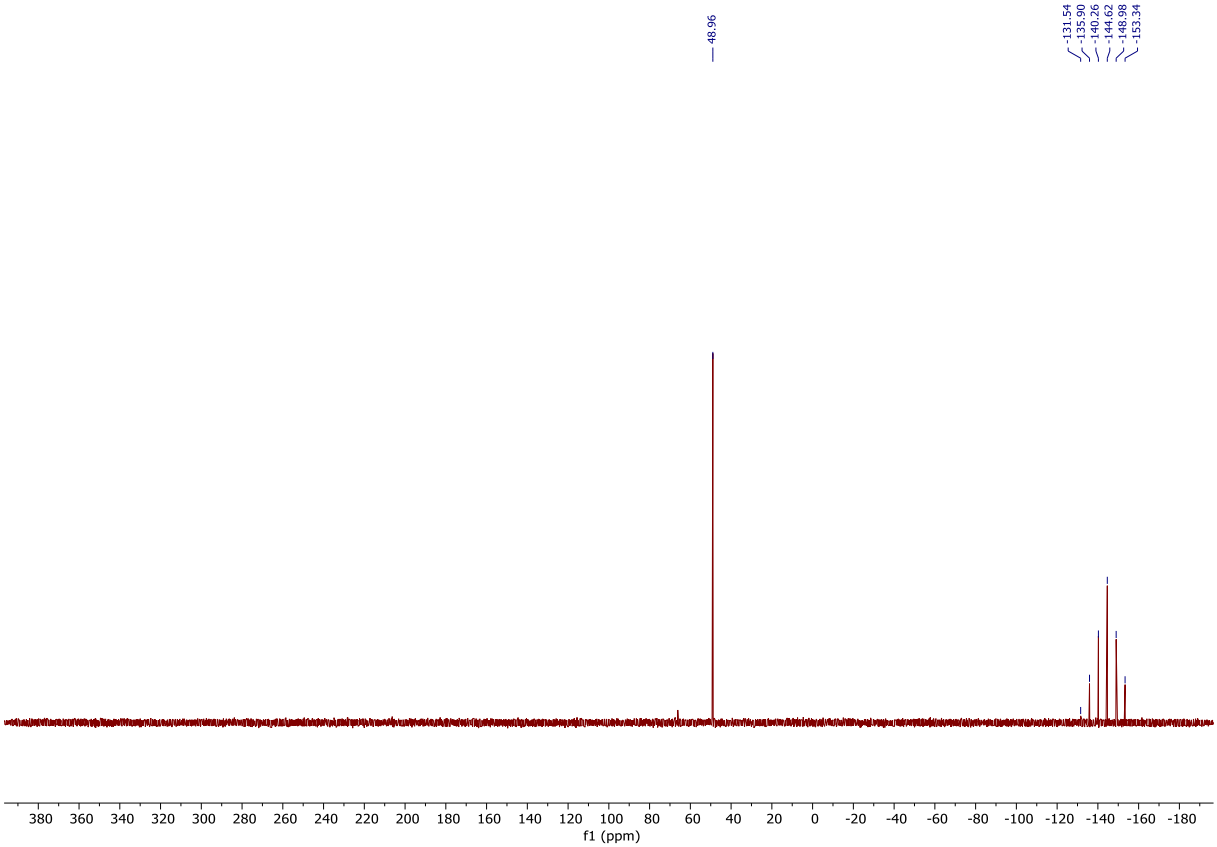

Figure S15. ^{31}P NMR of **3**[PF_6] (162 MHz, CD_3CN, 25°C)

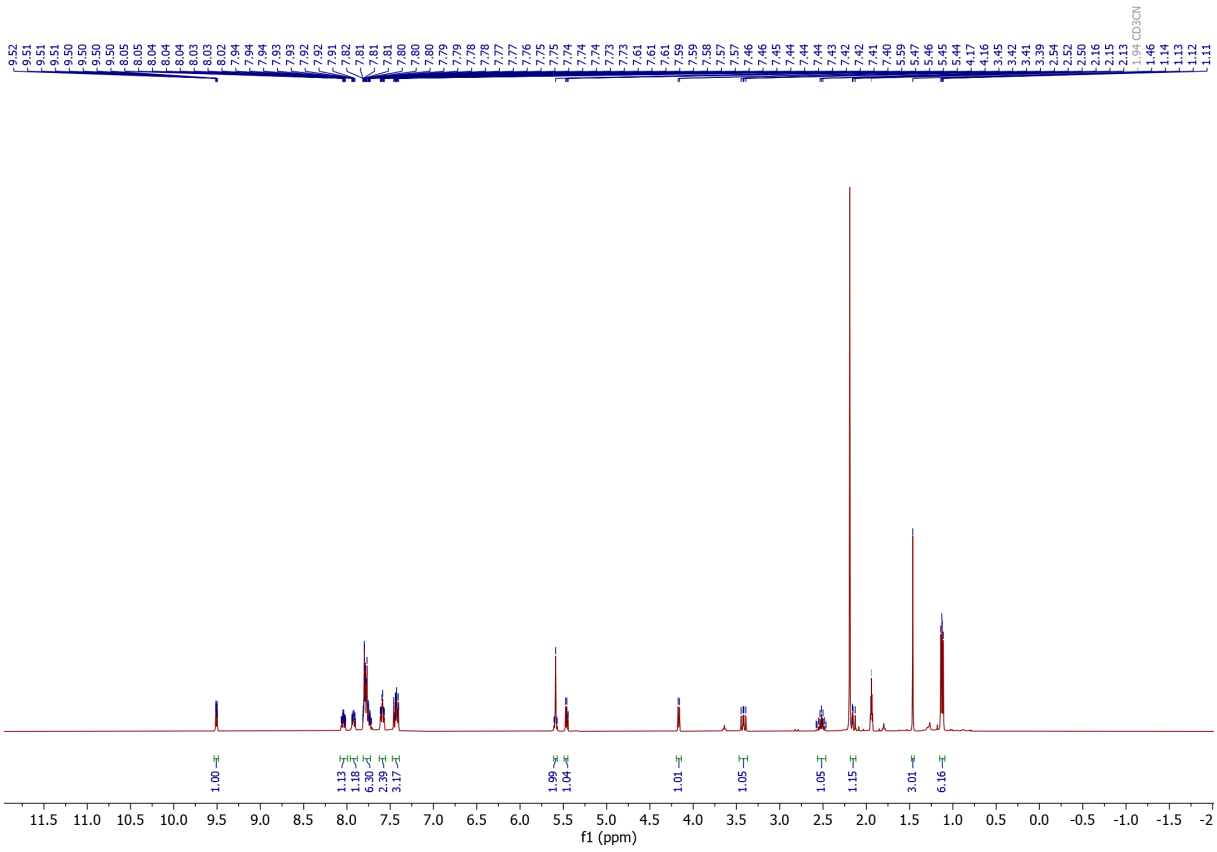

Figure S16. ^{1}H NMR of **3**[PF_6] (400 MHz, CD_3CN, 25°C)

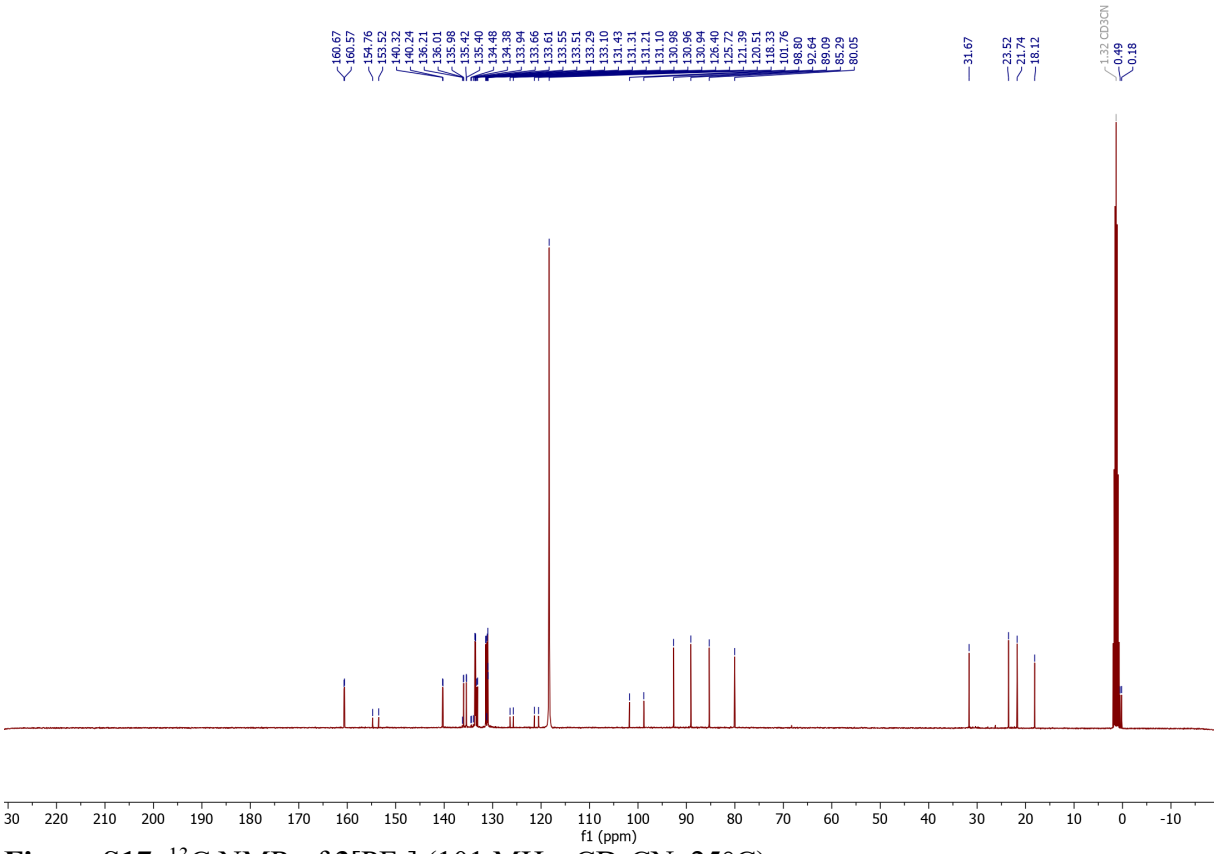

Figure S17. ^{13}C NMR of **3**[PF_6] (101 MHz, CD_3CN, 25°C)

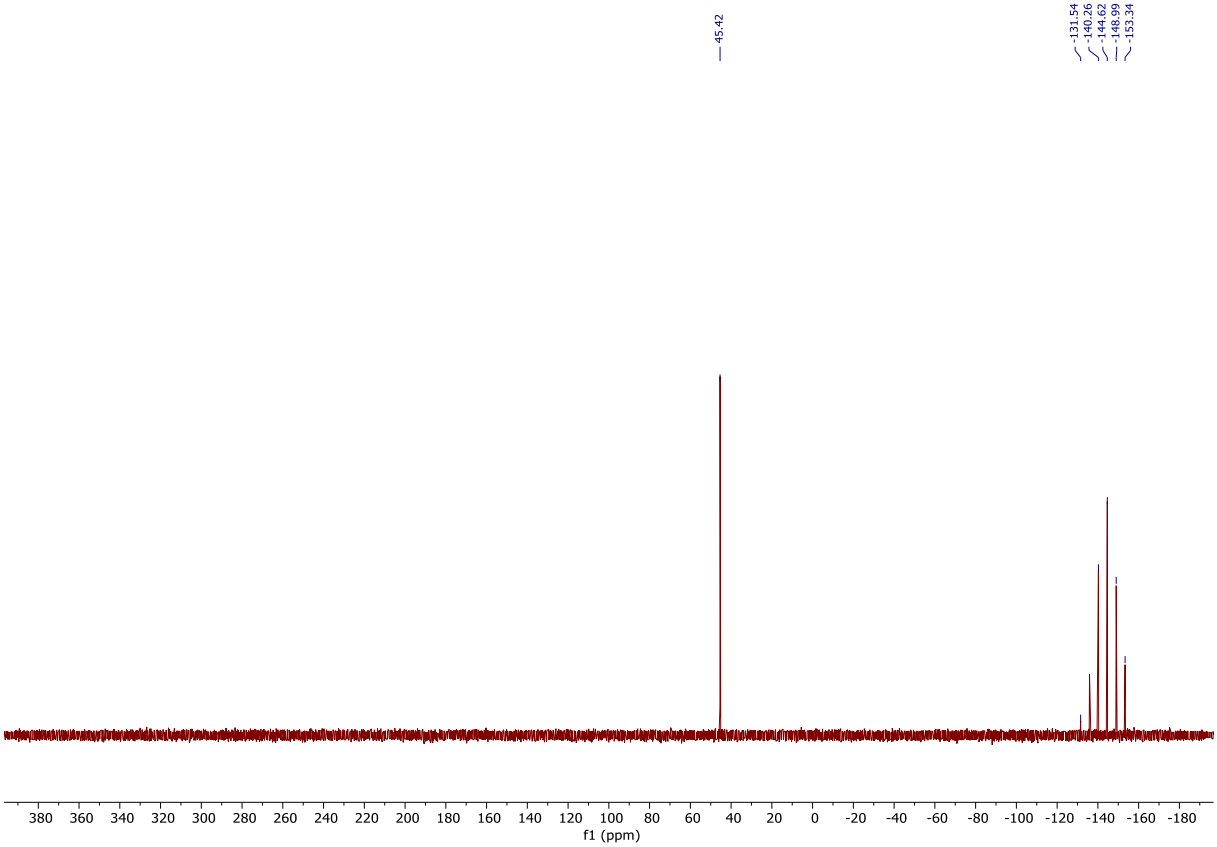

Figure S18. ^{31}P NMR of **C**[PF_6]$_2$ (162 MHz, CD_3CN, 25°C)

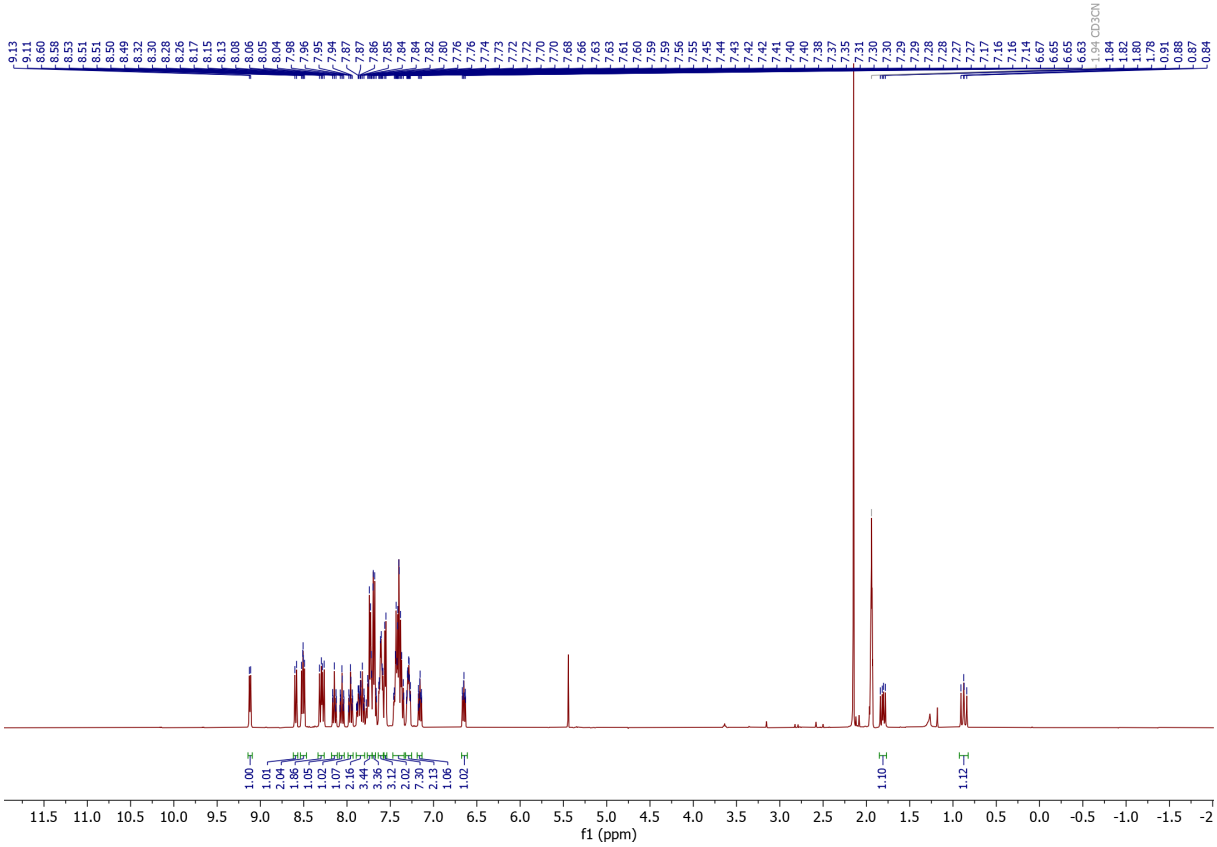

Figure S19. ^{1}H NMR of **C**$[PF_6]_2$ (400 MHz, CD_3CN, 25°C)

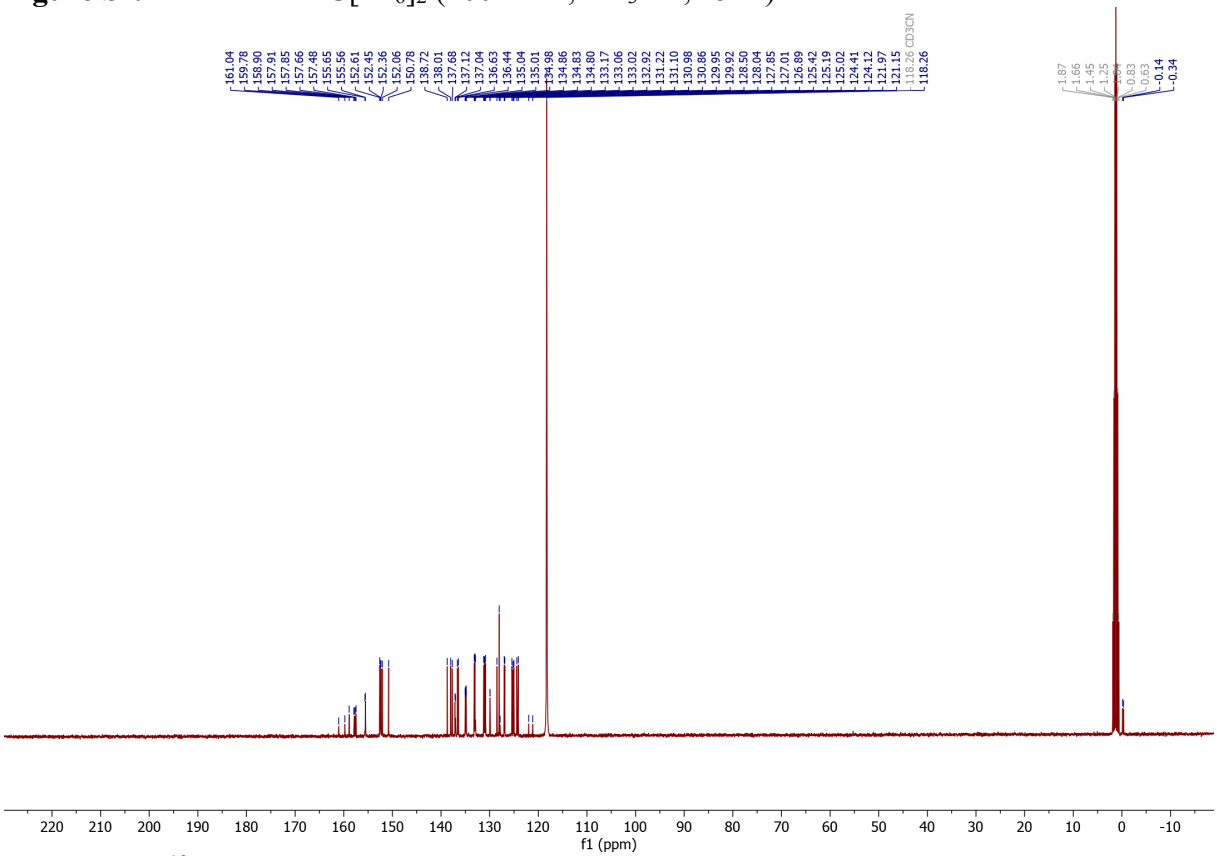

Figure S20. ^{13}C NMR of **C**$[PF_6]_2$ (101 MHz, CD_3CN, 25°C)

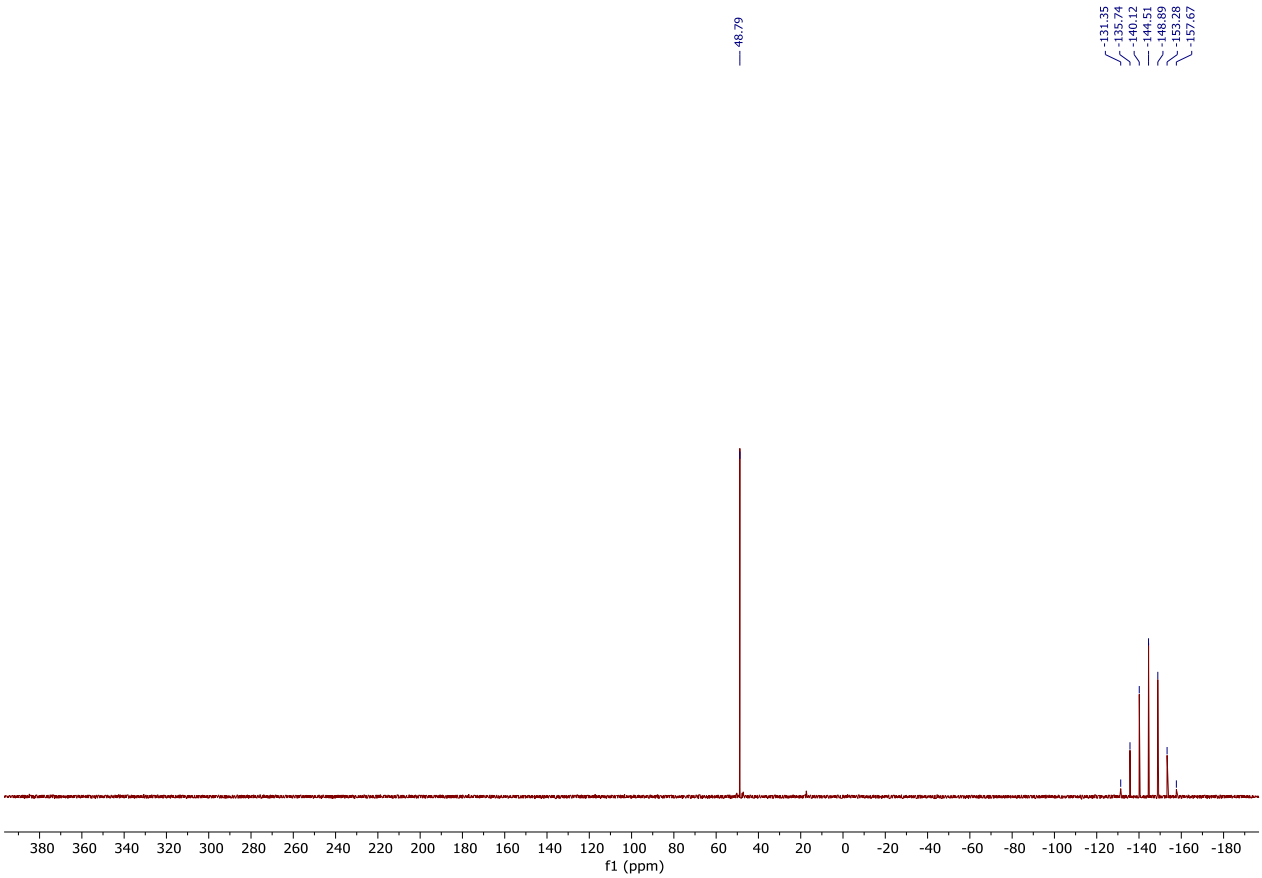

Figure S21. ^{31}P NMR spectrum of **4**$[PF_6]_2$ (162 MHz, CD_2Cl_2, 25°C)

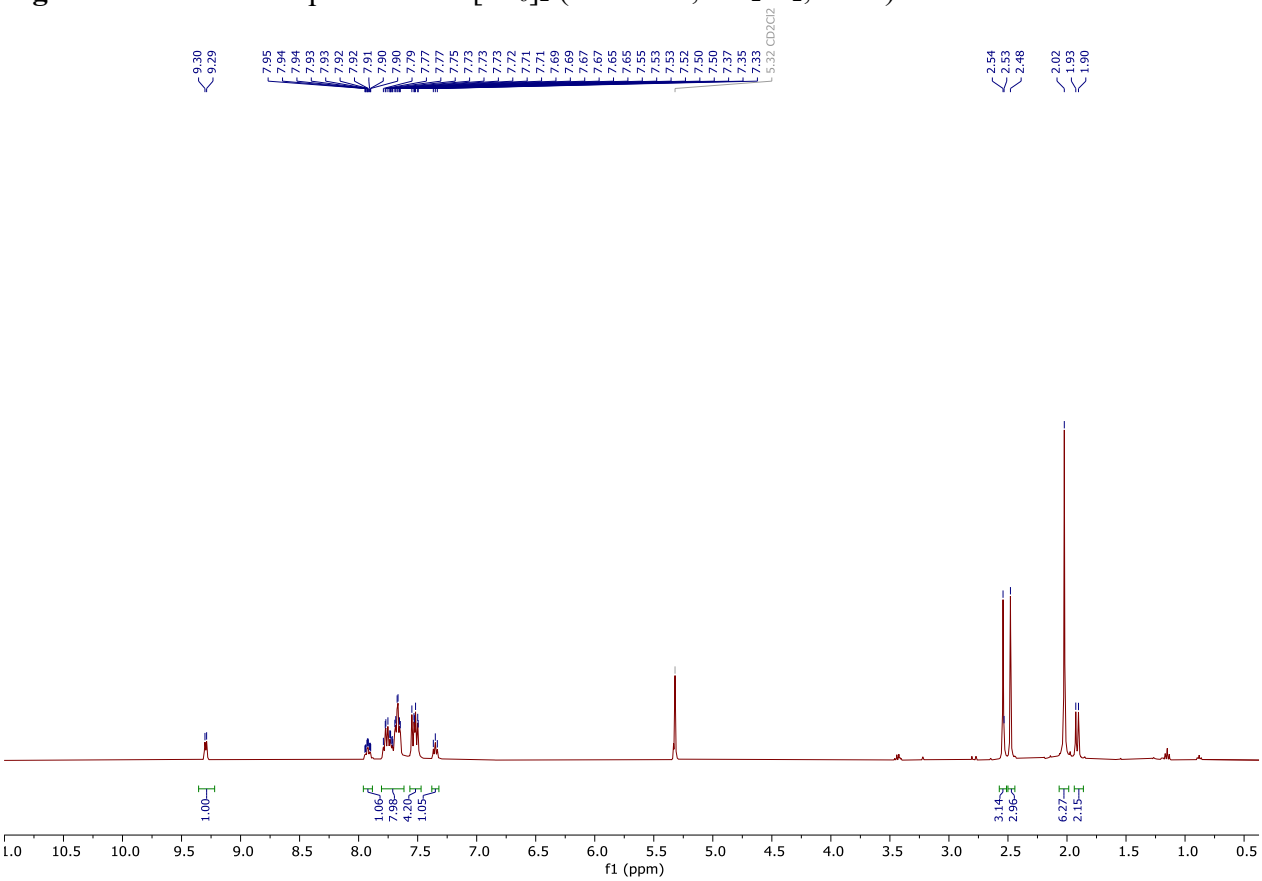

Figure S22. ^{1}H NMR of **4**$[PF_6]_2$ (400 MHz, CD_2Cl_2, 25°C)

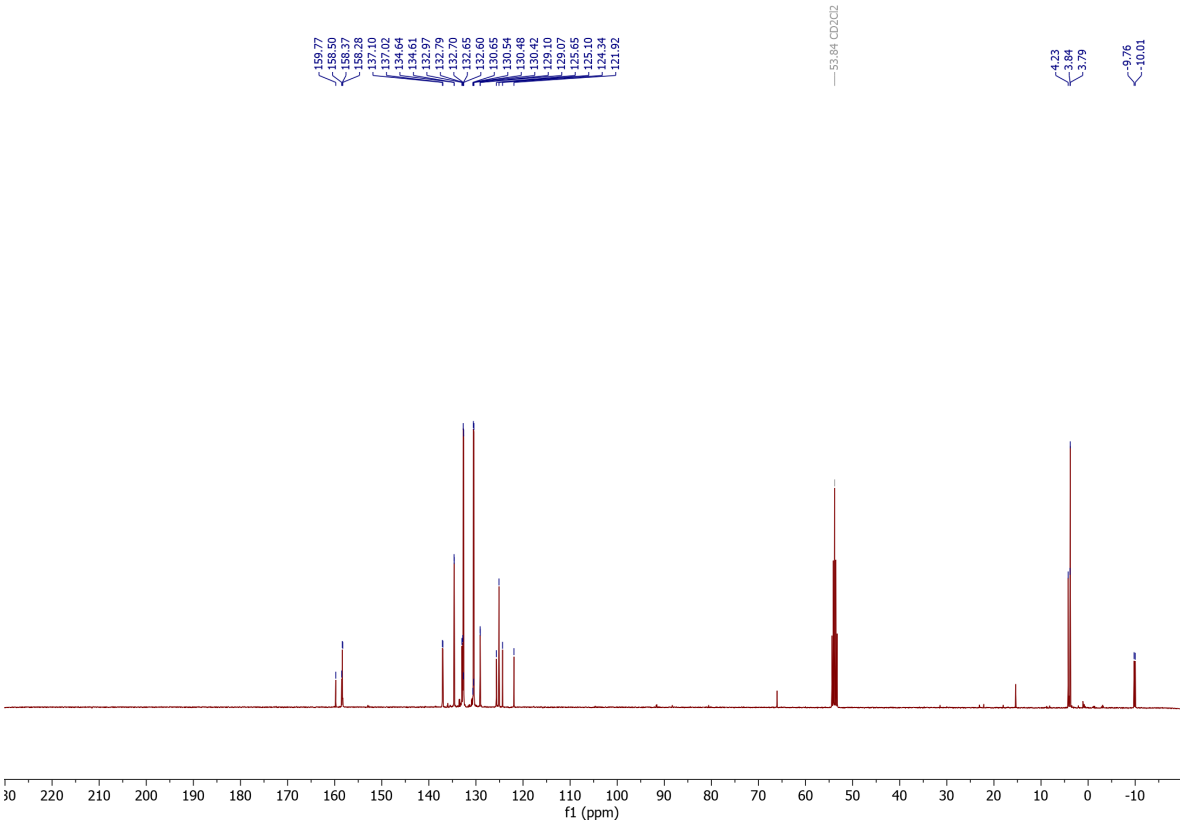

Figure S23. ^{13}C NMR spectrum of **4**$[PF_6]_2$ (101 MHz, CD_2Cl_2, 25°C)

IX) References

[1] J. Tönnemann, J. Risse, Z. Grote, R. Scopelliti and K. Severin, *Eur. J. Inorg. Chem*., 2013, 4558–4562.

[2] G. M. Sheldrick, *Acta Cryst*., 2015, **A71**, 3−8.

[3] L. Palatinus and G. Chapuis, *J. Appl. Cryst*., 2007, **40**, 786−790.

[4] P. W. Betteridge, J. R. Carruthers, R. I. Cooper, K. Prout and D. J. Watkin, *J. Appl. Cryst*., 2003, **36**, 1487.

[5] G. M. Sheldrick, *Acta Cryst*., 2008, **A64**, 112−122.

[6] A. L. Spek, *Acta Cryst. Sect. C.*, 2015, **71**, 9−18.

[7] F. Neese, F. Wennmohs, U. Becker and C. Riplinger, *J. Chem. Phys.,* 2020, **152**, 224108.

[8] F. Neese, *Wiley Interdiscip. Rev. Comput. Mol. Sci.,* 2012, **2**, 73–78.

[9] A. Becke, *J. Chem. Phys.,* 1993, **98**, 5648–5652.

[10] B. Mennucci, *Wiley Interdiscip. Rev. Comput. Mol. Sci.,* 2012, **2**, 386–404.

[11] T. Yanai, D. P. Tew and N. C. Handy, *Chem. Phys. Lett.,* 2004, **393**, 51–57.

[12] R. L. Martin, *J. Chem. Phys.,* 2003, **118**, 4775–4777.

[13] T. J. Penfold, E. Gindensperger, C. Daniel and C. M. Marian, *Chem. Rev*., 2018, **118**, 6975–7025.